A Nanomolar Multivalent Ligand as Entry Inhibitor of the Hemagglutinin of Avian Influenza

Moritz Waldmann,[†] Raffael Jirmann,[†] Ken Hoelscher,[†] Martin Wienke,[†] Felix C. Niemeyer,[†] Dirk Rehders,[‡] and Bernd Meyer*,[†]

[†]Department of Chemistry, University of Hamburg, 20146 Hamburg, Germany

[‡]Joint Laboratory for Structural Biology of Infection and Inflammation, Institute of Biochemistry and Molecular Biology, University of Hamburg and Institute of Biochemistry, University of Luebeck, c/o Deutsches Elektronen-Synchrotron (DESY), Notkestrasse 85, 22607 Hamburg, Germany

Ⓢ *Supporting Information*

ABSTRACT: Influenza virus attaches itself to sialic acids on the surface of epithelial cells of the upper respiratory tract of the host using its own protein hemagglutinin. Species specificity of influenza virus is determined by the linkages of the sialic acids. Birds and humans have $\alpha2-3$ and $\alpha2-6$ linked sialic acids, respectively. Viral hemagglutinin is a homotrimeric receptor, and thus, tri- or oligovalent ligands should have a high binding affinity. We describe the *in silico* design, chemical synthesis and binding analysis of a trivalent glycopeptide mimetic. This compound binds to hemagglutinin H5 of avian influenza with a dissociation constant of $K_D = 446$ nM and an inhibitory constant of $K_I = 15$ μM. *In silico* modeling shows that the ligand should also bind to hemagglutinin H7 of the virus that causes the current influenza outbreak in China. The trivalent glycopeptide mimetic and analogues have the potential to block many different influenza viruses.
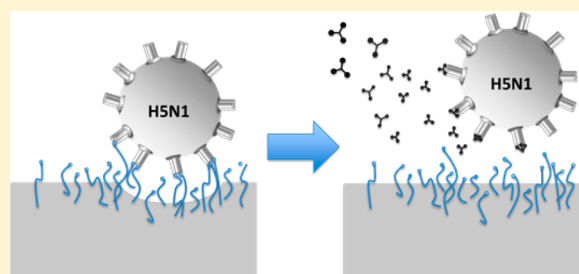
INTRODUCTION

Avian influenza has become a serious threat to human health. The infection is species specific and depends on the glycosidic linkage of the sialic acids in the upper respiratory tract. In the upper respiratory tract, humans have predominantly $\alpha2-6$ linked sialic acid carbohydrate moieties, while birds carry $\alpha2-3$ linked sialic acids. The surface protein hemagglutinin of influenza is either specific for $\alpha2-3$ linkages, e.g., H5 and H7, or $\alpha2-6$ linkages, e.g., H1, H2, H3.[1] The first outbreak of avian influenza was caused by a viral influenza strain that has the H5 hemagglutinin on its surface.[2] Infections of humans with avian flu have very recently been shown to also occur with viruses carrying the H7 hemagglutinin. This new virus found in China seems to be much more infectious to humans than the previous H5N1 virus. Furthermore, a highly pathogenic strain like H5N1 with a high mortality rate can undergo genetic reassortment with a strain that has an effective human-to-human transmission like the swine influenza H1N1. Those viruses would pose a serious pandemic threat.[3]

Antiviral therapeutics are available targeting two of the three major influenza virus surface proteins: the neuraminidase and the M2 ion channel.[4] No compound targeting the third protein, hemagglutinin, at the binding pocket has been approved as drug. However, small molecules inhibiting the membrane fusion by binding to the interface of the HA subunits have been developed.[5] An increasing number of resistant influenza strains makes the search for new therapeutics indispensable.[4c,6] The crystal structure of an influenza hemagglutinin was first published by Wiley et al. in 1981. It triggered an extensive search for small molecules with high affinity for hemagglutinin.[7] In fact, the search proved to be difficult, and despite the more than 30 years of search, no competitive inhibitor with therapeutic potential was found. This is due to the weak interaction of hemagglutinin to its natural ligand sialic acid.[8] The strong interaction between virus and host cell is caused by multivalent binding of the homotrimeric hemagglutinin molecules to the numerous carbohydrate moieties on the surface of the host cell.[9] Polymeric multivalent ligands were shown to exert tight binding to hemagglutinin.[10]

RESULTS AND DISCUSSION

Here we describe the *in silico* design, synthesis and *in vitro* analysis of a trivalent ligand that binds influenza hemagglutinin H5 of avian influenza in the high nanomolar range. As a species highly pathogenic to humans avian influenza is characterized by an unusual high mortality rate (~60%) compared to that of seasonal influenza (0.01–0.001%), we chose H5 of avian influenza as model system.[11] On the basis of the crystal structures of avian influenza H5 published in 2001 and 2006, we designed *in silico* ligands and calculated their binding energies.[12] The position of the binding pocket at the top of the globular domain distal to the virus membrane allowed the development of a trimeric structure with a centrally positioned
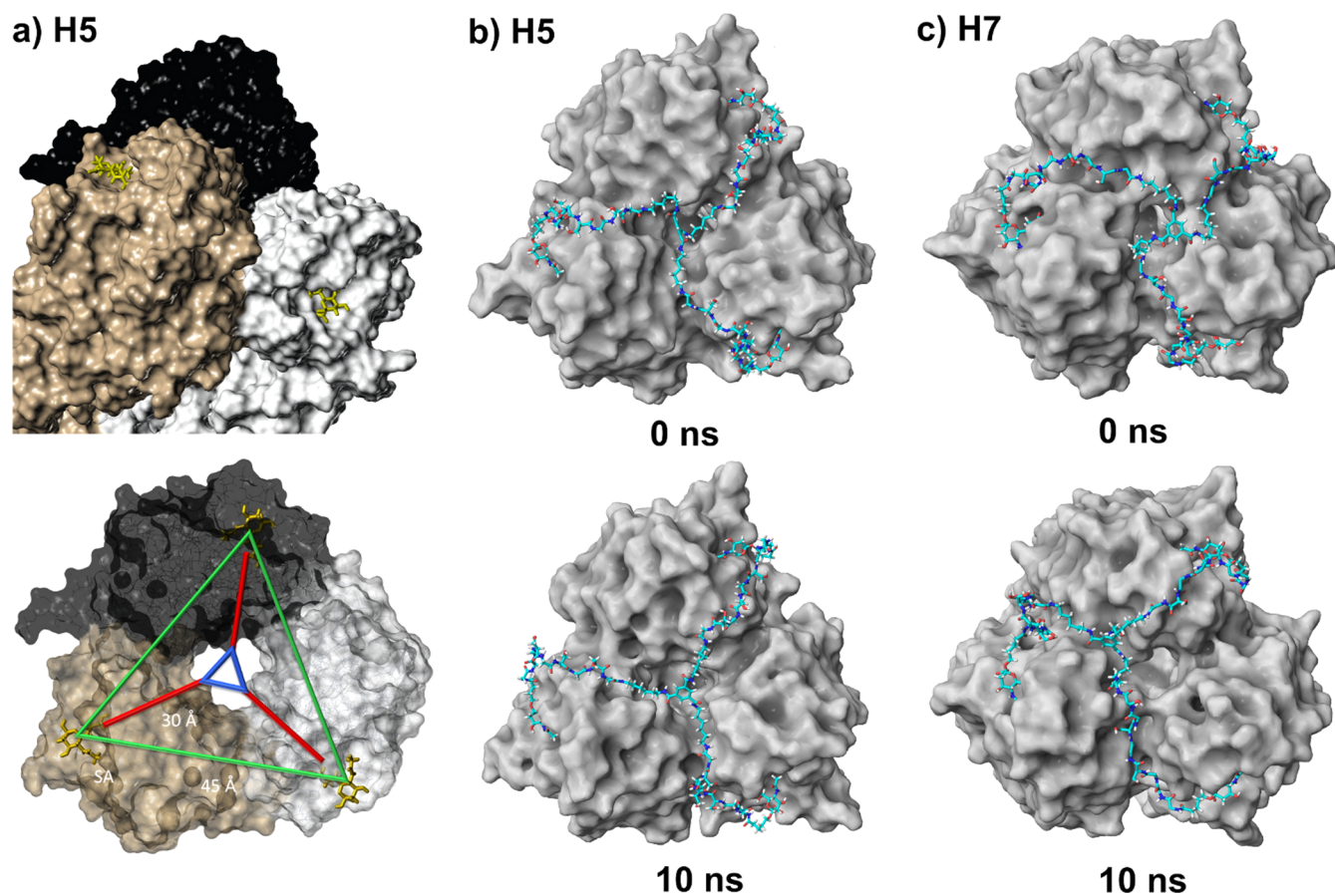
Figure 1. Crystal structures of H5 and H7 trimers shown as surface plots with ligands. (a) Sialic acids (yellow) in the binding pockets as determined in pdb 1JSO of hemagglutinin H5. The top of the globular domain, which is distal to the virus membrane, is shown. The hemagglutinin monomers are colored black, brown, and white, respectively. The exposed position of the binding site is predestinated for the development of a trimeric ligand with a centrally positioned core structure with radial topology. Top: view of the top of hemagglutinin shown at an angle. Bottom: view along the axis of the hemagglutinin H5 trimer with the distances between the binding sites highlighted. (b) View on top of hemagglutinin H5 with ligand **1** bound to all three binding sites at two different times of an MD simulation. The ligand is shown in atom colors. Flexibility during the dynamics simulation is predominantly found at the core while all three sialic acid residues remain in their binding pocket. (c) View on top of the hemagglutinin H7 (from pdb 3M5G) with ligand **1** bound to all three binding sites at two different times of an MD simulation. Motion is predominantly found at the core structure while all three sialic acid residues remain in their binding site during the simulation indicating that **1** is also a good ligand for H7.
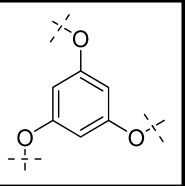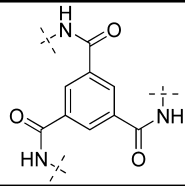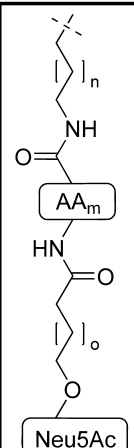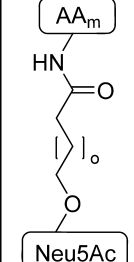
core which is connected to the three binding pockets (Figure 1a, top). The distance between the binding pocket and the symmetry axis of the trimer is approximately 30 Å (Figure 1a, bottom). The radial topology is optimal for hemagglutinin inhibitors because of the exposed position of the binding pockets and also thermodynamically favored over all other topologies as shown by Bundle et al.[13] Different types of scaffolds and the influence of structure and size regarding the same target were reviewed by Kiessling et al.[14]
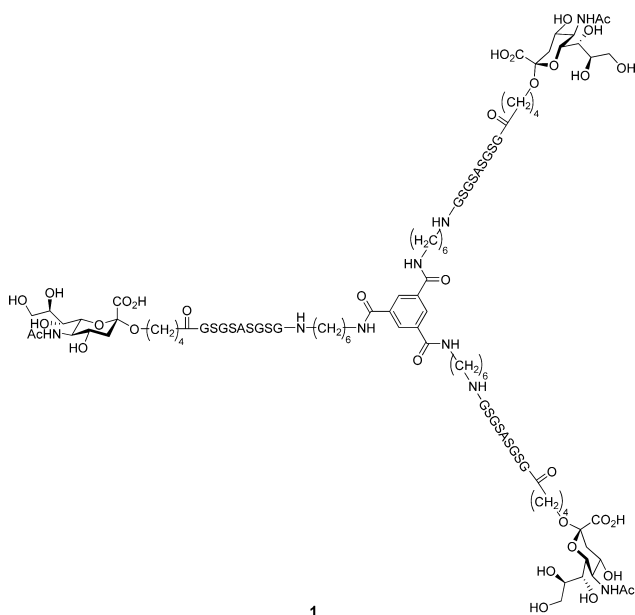
Structural as well as thermodynamic and entropic considerations led to the development of ligands with a core structure mimicking the C_3 symmetry of the protein. *In silico*, potential ligands with different core structures were derived from 1,3,5-alkoxycyclohexane, 1,3,5-alkoxybenzene or benzene-1,3,5-tricarboxylic acid (trimesic acid). The value of trimesic acid as scaffold for multivalent ligands was demonstrated by Whitesides and his group in his vancomycin studies.[15] In order to achieve water solubility, peptidic fragments as well as alkyl groups were integrated. The flexible alkyl chains act as spacers between the core and the more rigid peptide fragments and between the sialic acid and the peptide. We chose the flexible alkyl chains in two positions of the trimeric ligand to compensate a nonperfect steric match between ligand and

protein. Compared to often used ethylene glycol oligomers, a structurally well-defined peptide segment was introduced to reduce overall flexibility, which in turn reduces the entropic loss from conformational flexibility during binding. An alternating sequence of glycine and serine was chosen, which does not form a secondary structure as verified by CD-spectroscopy of the peptidic fragment 7 as well as of ligand **1**. This sequence is often being used as biocompatible linker in the construction of single chain antibodies and it is not intended to assist binding.[16] Alanine was introduced for practical reasons to facilitate NMR analysis by breaking the symmetry. The length of the peptide and of the alkyl linkers was varied and their binding energy was assessed by docking the corresponding structures into the binding sites and by calculating their binding energies. The optimized ligand complexes were used to identify structural requirements. A nine amino acid long peptide fragment gave the best energy. Shortening the peptide chain by one amino acid led to a significant loss of binding affinity. We could also obtain the optimal length of the alkyl chain proximal to the core structure. Six methylene groups yielded a flexible spacer between the aromatic core, i.e., trimesic acid, and the peptide linker. The sialic acid was also connected to the peptide linker by an alkyl chain with five carbon atoms. The docking results

for ligands with 1,3,5-trihydroxybenzene and trimesic acid derived cores are shown in Table 1 (for an extended version including also *cis,cis*-1,3,5-trihydroxy-cyclohexane see Table S1). To compensate the reduced flexibility of the amide bond of the trimesic acid core, we elongated the adjacent alkyl chain by one methylene group for this ligand for direct comparison. Some

Table 1. Summary of the *in Silico* Results[a]

	calc. bind. energy [kcal/mol]		calc. bind. energy [kcal/mol]
n = 3 m = 8 o = 1	8.5	n = 4 m = 8 o = 1	18.0
n = 3 m = 8 o = 2	15.7	n = 4 m = 8 o = 2	17.0
n = 3 m = 9 o = 2	1.3	n = 4 m = 9 o = 2	0.0 ligand 1
n = 2 m = 9 o = 2	2.3	n = 3 m = 9 o = 2	3.4
n = 4 m = 9 o = 2	1.1	n = 5 m = 9 o = 2	4.4

1

[a]Different peptidic linker length (*m*) and alkyl chain length (*n* and *o*) were docked and binding energies were calculated. The energies are expressed relative to the ligand with the best binding energy. The structure of ligand **1** is shown at the bottom of the table. The ligand consists of a trimesic acid derived core structure which is bound by flexible hexyl chains to the nonapeptide linkers. The sialic acid epitope is bound by a flexible alkyl chain to the N-terminus of the peptidic linker.

cyclohexyl containing ligands yielded similar binding energies, i.e., +0.2 and 1.1 kcal/mol, respectively. Due to the complexity of modeling the interaction of a trivalent ligand with trimeric protein, the calculated energies are considered to be estimates of the respective real binding energy. For obvious reasons, we decided to synthesize the ligand with the best predicted energy. We also wanted to synthesize the 1,3,5-trihydroxy-benzene derived ligand with the best predicted energy (Table 1). However, because of low yields in derivatizing the 1,3,5-trihydroxy-benzene as core, we focused on the trimesic acid core.[17]

After orienting chemistry, we synthesized ligand **1** with the trimesic acid derived core structure, a hexyl side chain, a nine amino acid long peptide sequence, another pentyl alkyl chain and a sialic acid glycoside (cf. structure in Table 1, bottom). The aromatic core and the anomeric center of the sialic acid are spaced by 42 bonds to bridge the distance of 30 Å and enable simultaneously binding of all three sialic acids. This was verified by a 10 ns molecular dynamic (MD) simulation of the protein/ligand complex in a water box using Desmond as part of the Schrödinger suite. During the MD a small amount of movement was observed for the core while all three sialic acids remained in their respective binding pocket over the full simulation (Figure 1b; also watch movie 1 in Supporting Information). The complex of ligand **1** with H5 was analyzed showing dominantly interactions between the sialic acid and H5, which are similar to the binding mode of sialic acid to H5 in the crystal.[12a] Thus, the pose of the three sialic acids in ligand **1** when docked to H5 is almost identical to that of the sialic acids in the X-ray structure with the NHAc function and the glycerol side chain in close proximity to the protein (Figure 1b; for a ligand-interaction plot see Figure S1 in Supporting Information). We also find few interactions of the pentyl chain and the two N-terminal amino acids with H5.

Ligand **1** was synthesized by a convergent approach. The sialic acid chloride acting as glycosyl donor for the synthesis of building block **5** was prepared by standard procedure[18] and glycosylated with 5-hexene-1-ol, which in turn was oxidized under cleavage of the terminal double bond by ruthenium(III) chloride yielding building block **5**, which was also used for synthesis of **6** (Figure 2a). Synthesis of the peptide was carried out by standard protocol for microwave assisted automated SPPS. Sialic acid building block **5** was coupled to the nascent peptide on solid support. Glycoconjugate **8** was cleaved from the resin with simultaneous removal of all protecting groups of the peptide side chain. This was essential to ensure solubility and allowing purification of the compounds. Compound **3** was reacted with **8** to give the trivalent glycoconjugate **10**. The latter two reactions are very sensitive to the excess and concentration of **5** and **8**, respectively. Final deprotection led to **1** which was purified by RP-HPLC (Figure 2c). We synthesized fragments of **1** to test the binding affinity and the effect of multivalency. Compound **9** was prepared as monovalent fragment of **1** from compound **8**, which was also used for the synthesis of **1**. Additionally, compounds **6** and **7** were prepared as fragments of **1** (Figure 2b,c). All compounds were characterized for their binding affinity.

For the experimental binding studies, trimeric H5 (A/Vietnam/1203/2004) was used. The thermodynamic dissociation constant K_D was determined by surface plasmon resonance (SPR) on a Biacore T100 immobilizing hemagglutinin to the sensor chip. Evaluation of the SPR data using the 1:1 binding model yielded K_D = 450 nM (Figure 3, top). Compared to
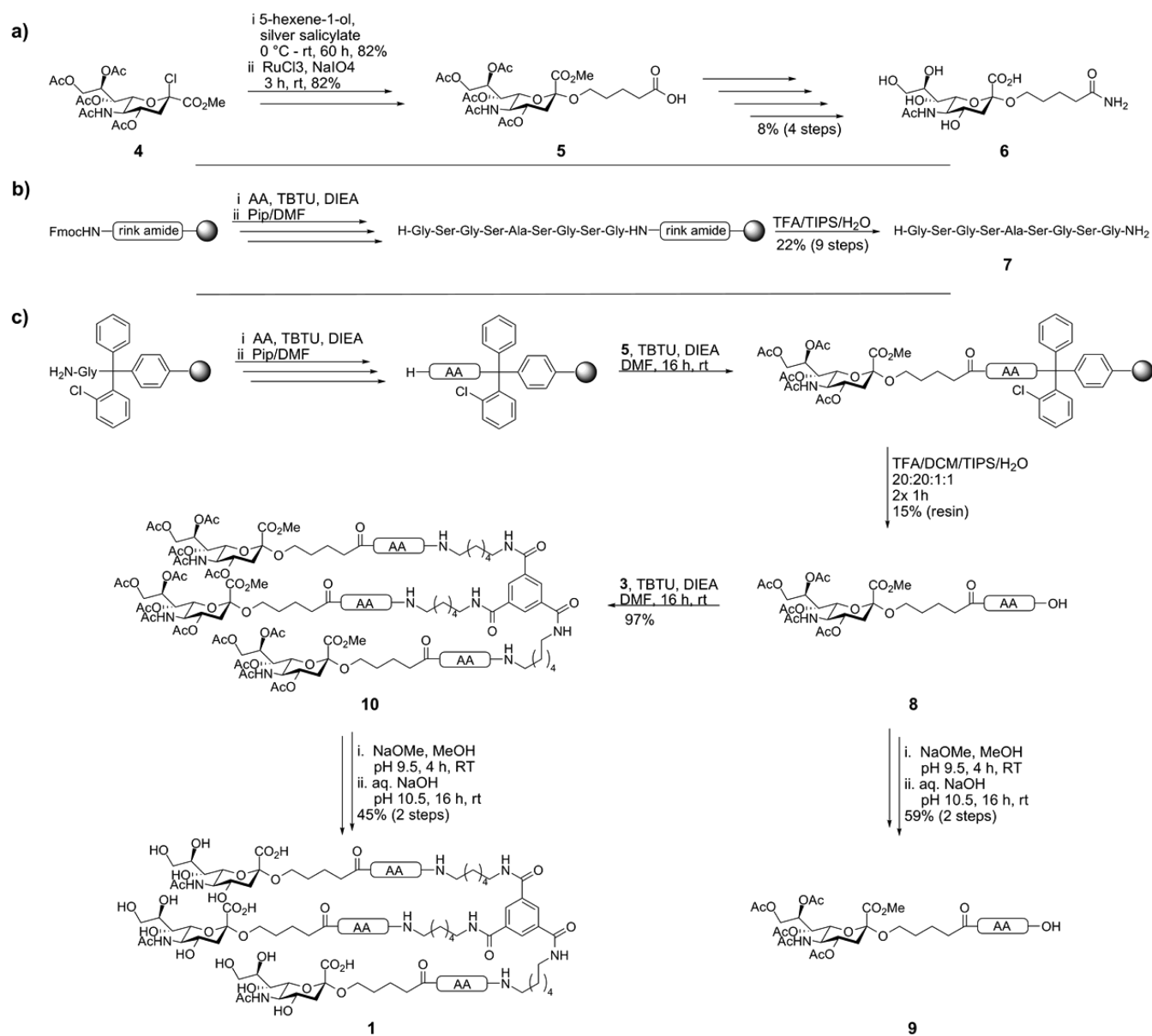
Figure 2. Synthesis of ligand **1**: (a) synthesis of building block **5**[19] that was also used for synthesis of fragment **6**; (b) synthesis of the peptide fragment by standard protocol for microwave assisted solid phase peptide synthesis; (c) synthesis of ligand **1** using building blocks **3** and **5**. For synthesis of compound **3**, see Supporting Information.

Neu5Acα2Me, the affinity was increased by a factor of 4000. For a bivalent interaction, one would expect an increase of a factor of about 500 and for a trivalent interaction a factor of ~300 000. Thus, we reached an interaction strength that is between bi- and trivalency. Reported avidities of multivalent ligands for influenza hemagglutinin show enhanced binding relative to the methyl sialoside by a factor of 100 for a bivalent molecule[20] up to a factor of 1 000 000[10] for polymeric substrates. One of the first synthetic bivalent ligands was reported by Knowles et al. and had an 100-fold increased affinity against whole viruses in a hemagglutination assay when compared to Neu5Acα2Me. Interestingly, the bivalent ligand did not bind to bromelain-released hemagglutinin because of unknown reasons as a cross-linking of viruses was due to the low viral concentration excluded.[20] Roy and co-workers were one of the first to report higher multivalent ligands derived from synthetic sialylated glycoconjugates, which reduced viral infectivity by a factor of 130.[21] The tightest binding of a

sialylated polymer was reported by Whitesides et al. with an increased binding of up to 1 000 000 compared to Neu5-Acα2Me as assessed from IC_{50} values determined in an ELISA assay.[10] Unfortunately, much of this exciting research was not continued, mainly due to an insufficient binding or the high molecular weight and most importantly polymeric derivatives of sialic acid will likely bind to all receptors for sialic acids and thus have a low specificity. Here, we demonstrate the power of custom tailored ligands for influenza hemagglutinin.

We also used STD-NMR studies with α-methyl sialoside (Neu5Acα2Me) as competitor to determine inhibition constants.[22] For competitive studies, a 0.55 μM solution of H5 trimer containing 20 mM Neu5Acα2Me was used. Ligand **1** was added stepwise to this solution to a final concentration of 150 μM (micelle formation was observed at higher concentrations as verified by dynamic light scattering measurements). The absolute STD% for each competitor proton signal was plotted against the logarithm of the ligand concentration
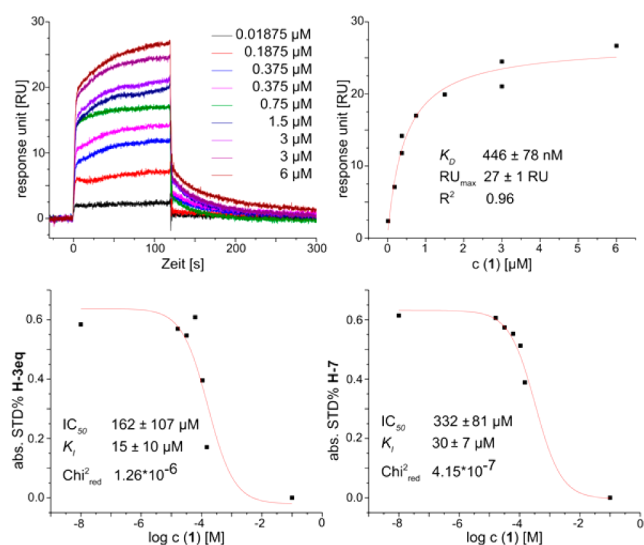
Figure 3. Top: SPR sensorgram (left) and analysis (right) of ligand **1**. H5 was immobilized on sensor chip and concentrations of **1** from 0.019 to 6 μM were measured. Thermodynamic analysis yielded a K_D = 446 nM. Bottom: results from competitive STD-NMR experiments. To a solution of 20 mM Neu5Acα2Me and 0.55 μM H5 in PBS, ligand **1** was titrated to a final concentration of 150 μM. The STD-NMR signals of the competitor were integrated and plotted against the logarithm of the ligand concentration to yield IC_{50} = 162 μM and K_I = 15 μM using the signal of H-3eq of sialic acid (left) and IC_{50} = 332 μM and K_I = 30 μM using the signal of H-7 (right).

and the data points were fitted to the one site competition model yielding the IC_{50} value (Figure 3, bottom). Ligand **1** was able to displace Neu5Acα2Me from the primary carbohydrate recognition domain. The IC_{50} values for the competitor were determined and converted into the inhibition constant K_I using the Cheng-Prusoff equation.[23] K_I values in the low micromolar range with a good homogeneity were obtained with K_I = 15 μM using H-3eq of Neu5Acα2Me. The multivalent effect was proven by comparing the inhibition constant of **1** with that of the monovalent fragment **9**, which showed no competitive behavior in the STD measurements (Figure S9). It is important to prove that the interaction is of a multivalent nature to further development of this concept toward medical applications.

To analyze the structural influences of the multivalent effect, a small substance library was synthesized. Analogs of **1** with 9, 10, and 11 amino acids (ligands **11−14**, Figure S16) and also with a shortened spacer to the aromatic core using a C4 diamine were prepared. None of these compounds performed better than compound **1** (Figure S5−S8 and S10−S13). The thermodynamic binding constants of these derivatives of **1** were in the low millimolar range. This shows clearly that no multivalent effect is operative for the molecules **11-14**. More importantly, in competition assays, these ligands have no inhibitory activity for the primary binding site of hemagglutinin. This is further demonstrated by analysis of the monovalent fragment **9** which has almost identical binding properties as the trimeric ligands **11−14**. The structural properties of ligand **1** seem to match the geometry of hemagglutinin extremely well, such that even slightly modified spacers show no multivalency: We observed drastically worse interaction in constructs that have shortened spacers. Molecules elongated in the peptide chain are also worse binders than **1**. Even with nine amino acids in the peptide chain we find that the alkyl chains cannot be made shorter without losing significant amounts of the binding affinity (cf. Supporting Information).

Ligand **1** utilizes only the binding sites of the sialic acids on the trimeric hemagglutinin. Therefore, we hypothesized that the trimeric compound **1** and possibly analogs of this compound are generically able to interact with most influenza hemagglutinins, which are all trimeric. In the current outbreak of avian flu in China, the virus utilizes another hemagglutinin, H7. Therefore, we tested *in silico* whether compound **1** would be able to bind to H7. In a docking experiment and a molecular dynamics simulation with trimeric H7 (pdb 3M5G),[24] we found that compound **1** is well capable to also block hemagglutinin H7. During the 10 ns MD-simulation, all three sialic acids of ligand **1** remained in the binding pockets of hemagglutinin while flexibility was found among the alkyl chains and the peptidic fragment (Figure 1c; also see movie 2 in Supporting Information). This is an indicator that ligand **1** might have a very broad activity to various hemagglutinins.

For further development toward a drug for use in a pandemic situation, more questions need to be addressed. One important question is the bioavailability. As the target location, i.e., the upper respiratory tract, is easily accessible, the molecule can be applied as an aerosol as a delivery method. Thus, commonly asked pharmacokinetic delivery issues are not relevant for this molecule.

A decay of the molecule by the viral neuraminidase is, for several reasons, unlikely. First, the high specific avidity for hemagglutinin reduces the local concentration of the molecule in close proximity to the neuraminidase drastically. Second, the relatively low efficiency (k_{cat} = 9 s^{-1}) of neuraminidase makes a cleavage of sialic acids from **1** less likely. Third, only about 5−10% of the viral surface proteins are neuraminidases.[25] Furthermore, there is an ongoing discussion about the function of the influenza neuraminidase in primarily infection and the activation of the hydrolase activity.[26] Fourth, Knowles and co-workers did not observe a decay of their sialic acid containing ligands in a hemagglutination assay with whole viruses.[20] Current research in our group addresses questions of improving avidity and ease of synthesis before the present concept will be tested in *in vivo* studies.

■ CONCLUSION

Ligand **1** has a K_D in the high nanomolar range and is therefore a compound with one of the best reported affinities for small molecules exhibiting a clear multivalent effect.[27] This concept of a trimeric entry inhibitor can easily be modified and adapted to other viruses as new species arise as all influenza viruses have a trimeric hemagglutinin. The ligand presented here can interact with H5 and *in silico* also with H7 and, thus, has the potential to block the virus present in the current infection outbreak in China. In summary, we believe that the multimeric concept is a powerful tool especially for easily accessible body regions like the upper respiratory tract, where the application of an aerosol is possible and pharmacokinetic effects are less important. Because the binding epitope for all hemagglutinins, i.e., sialic acid, is determined by the host and because of the global nature of the multivalent interaction, these ligands are less prone to a viral escape by genetic drift and can also be easily structurally adjusted by simple modification of single building blocks and represent, therefore, a precious tool in order to develop powerful and long lasting drugs.

ASSOCIATED CONTENT

S Supporting Information

Details about the *in silico* data, a ligand interaction plot between H5 and **1**, SPR and STD-NMR data of all ligands and experimental procedures for the synthesis of the building blocks and the ligands; two 2 ns movies of the 10 ns molecular dynamic simulations of ligand **1** with H5 (movie1.qt) and with H7 (movie2.qt). This material is available free of charge via the Internet at http://pubs.acs.org.

AUTHOR INFORMATION

Corresponding Author

bernd.meyer@chemie.uni-hamburg.de

Notes

The authors declare no competing financial interest.

ACKNOWLEDGMENTS

REFERENCES

(1) Stevens, J.; Blixt, O.; Tumpey, T. M.; Taubenberger, J. K.; Paulson, J. C.; Wilson, I. A. *Science* **2006**, *312* (5772), 404−410.

(2) Salomon, R.; Webster, R. G. *Cell* **2009**, *136* (3), 402−410.

(3) Webby, R. J.; Webster, R. G. *Science* **2003**, *302* (5650), 1519−1522.

(4) (a) von Itzstein, M. *Nat. Rev. Drug Discovery* **2007**, *6* (12), 967−974. (b) Dyason, J. C.; von Itzstein, M. *Microbial Glycobiology*; Academic Press: Boston, MA, 2010; pp 269−283; (c) Lee, S. M.-Y.; Yen, H.-L. *Antivir. Res.* **2012**, *96* (3), 391−404.

(5) (a) Bodian, D. L.; Yamasaki, R. B.; Buswell, R. L.; Stearns, J. F.; White, J. M.; Kuntz, I. D. *Biochemistry* **1993**, *32* (12), 2967−2978. (b) Russell, R. J.; Kerry, P. S.; Stevens, D. J.; Steinhauer, D. A.; Martin, S. R.; Gamblin, S. J.; Skehel, J. J. *Proc. Natl. Acad. Sci. U.S.A.* **2008**, *105* (46), 17736−17741.

(6) (a) Le, Q. M.; Kiso, M.; Someya, K.; Sakai, Y. T.; Nguyen, T. H.; Nguyen, K. H.; Pham, N. D.; Ngyen, H. H.; Yamada, S.; Muramoto, Y.; Horimoto, T.; Takada, A.; Goto, H.; Suzuki, T.; Suzuki, Y.; Kawaoka, Y. *Nature* **2005**, *437* (7062), 1108. (b) van der Vries, E.; Stelma, F. F.; Boucher, C. A. B. *New Engl. J. Med.* **2010**, *363* (14), 1381−1382. (c) Yang, J.; Li, M.; Shen, X.; Liu, S. *Viruses* **2013**, *5* (1), 352−373.

(7) Wilson, I. A.; Skehel, J. J.; Wiley, D. C. *Nature* **1981**, *289* (5796), 366−373.

(8) Sauter, N. K.; Bednarski, M. D.; Wurzburg, B. A.; Hanson, J. E.; Whitesides, G. M.; Skehel, J. J.; Wiley, D. C. *Biochemistry* **1989**, *28* (21), 8388−8396.

(9) Mammen, M.; Choi, S.-K.; Whitesides, G. M. *Angew. Chem., Int. Ed.* **1998**, *37* (20), 2754−2794.

(10) Sigal, G. B.; Mammen, M.; Dahmann, G.; Whitesides, G. M. *J. Am. Chem. Soc.* **1996**, *118* (16), 3789−3800.

(11) Thompson, M. G.; Shay, D. K.; Zhou, H.; Bridges, C. B.; Cheng, P. Y.; Burns, E.; Bresee, J. S.; Cox, N. J. *J. Am. Med. Assoc.* **2010**, *304* (16), 1778−1780.

(12) (a) Ha, Y.; Stevens, D. J.; Skehel, J. J.; Wiley, D. C. *Proc. Natl. Acad. Sci. U.S.A.* **2001**, *98* (20), 11181−11186. (b) Yamada, S.; Suzuki, Y.; Suzuki, T.; Le, M. Q.; Nidom, C. A.; Sakai-Tagawa, Y.; Muramoto, Y.; Ito, M.; Kiso, M.; Horimoto, T.; Shinya, K.; Sawada, T.; Usui, T.; Murata, T.; Lin, Y.; Hay, A.; Haire, L. F.; Stevens, D. J.; Russell, R. J.; Gamblin, S. J.; Skehel, J. J.; Kawaoka, Y. *Nature* **2006**, *444* (7117), 378−382.

(13) (a) Kitov, P. I.; Bundle, D. R. *J. Am. Chem. Soc.* **2003**, *125* (52), 16271−16284. (b) Kitov, P. I.; Sadowska, J. M.; Mulvey, G.; Armstrong, G. D.; Ling, H.; Pannu, N. S.; Read, R. J.; Bundle, D. R. *Nature* **2000**, *403* (6770), 669−672.

(14) Gestwicki, J. E.; Cairo, C. W.; Strong, L. E.; Oetjen, K. A.; Kiessling, L. L. *J. Am. Chem. Soc.* **2002**, *124* (50), 14922−14933.

(15) Rao, J.; Lahiri, J.; Isaacs, L.; Weis, R. M.; Whitesides, G. M. *Science* **1998**, *280* (5364), 708−711.

(16) Shen, Z.; Yan, H.; Zhang, Y.; Mernaugh, R. L.; Zeng, X. *Anal. Chem.* **2008**, *80* (6), 1910−1917.

(17) Boland, Y.; Hertsens, P.; Marchand-Brynaert, J.; Garcia, Y. *Synthesis* **2006**, *9*, 1504−1512.

(18) (a) Kuhn, R.; Lutz, P.; Macdonald, D. L. *Chem. Ber.* **1966**, *99* (2), 611−617. (b) Furuhata, K.; Anazawa, K.; Itoh, M.; Shitori, Y.; Ogura, H. *Chem. Pharm. Bull.* **1986**, *34* (7), 2725−2731.

(19) Toogood, P. L.; Galliker, P. K.; Glick, G. D.; Knowles, J. R. *J. Med. Chem.* **1991**, *34* (10), 3138−3140.

(20) Glick, G. D.; Knowles, J. R. *J. Am. Chem. Soc.* **1991**, *113* (12), 4701−4703.

(21) Gamian, A.; Chomik, M.; Laferrière, C. A.; Roy, R. *Can. J. Microbiol.* **1991**, *37* (3), 233−237.

(22) (a) Mayer, M.; Meyer, B. *Angew. Chem., Int. Ed.* **1999**, *38* (12), 1784−1788. (b) Meyer, B.; Peters, T. *Angew. Chem., Int. Ed.* **2003**, *42* (8), 864−890.

(23) Cheng, Y.; Prusoff, W. H. *Biochem. Pharmacol.* **1973**, *22* (23), 3099−3108.

(24) Yang, H.; Chen, L.-M.; Carney, P. J.; Donis, R. O.; Stevens, J. *PLoS Pathog.* **2010**, *6* (9), e1001081.

(25) Janakiraman, M. N.; White, C. L.; Laver, W. G.; Air, G. M.; Luo, M. *Biochemistry* **1994**, *33* (27), 8172−8179.

(26) (a) Matrosovich, M. N.; Matrosovich, T. Y.; Gray, T.; Roberts, N. A.; Klenk, H. D. *J. Virol.* **2004**, *78* (22), 12665−12667. (b) Ohuchi, M.; Asaoka, N.; Sakai, T.; Ohuchi, R. *Microbes Infect.* **2006**, *8* (5), 1287−1293.

(27) (a) Song, G.; Yang, S.; Zhang, W.; Cao, Y.; Wang, P.; Ding, N.; Zhang, Z.; Guo, Y.; Li, Y. *J. Med. Chem.* **2009**, *52* (23), 7368−7371. (b) Weinhold, E. G.; Knowles, J. R. *J. Am. Chem. Soc.* **1992**, *114* (24), 9270−9275.

788

dx.doi.org/10.1021/ja410918a | *J. Am. Chem. Soc.* 2014, 136, 783−788